respectively, reproduce the heavy lined threshold curves in Figure 7. The dashed lines show v_2 and v_2' for conjugate phases in the monodisperse system as functions of the axis ratio x. Values of the disorder parameter for the respective systems, also shown in Figure 9, are similar. The dashed lines for v_2' and v_2 for monodisperse systems fall between those for the Poisson distribution for finite values of the (mean) axis ratio. As expected, the biphasic gap measured by the vertical distance between the pair of curves is greater for the Poisson distribution than for the monodisperse system with $x = \bar{x}_n^0$. With increase in $\bar{x}_n^0$ this difference diminishes. The curves for v_2 converge as $\bar{x}_n^0 \rightarrow \infty$; the curves for v_2' also converge, although somewhat more slowly. Hence, the ratio v_2'/v_2, representing the ratio of the phase gap concentrations, proceeds to the common limit, 1.5923.[1,4] Thus, the phase behavior for the Poisson distribution converges to that for the monodisperse solute as x increases. This is, of course, consistent with the diminishing relative breadth of the Poisson distribution with increase in its mean.

Acknowledgment. This work was supported by the Directorate of Chemical Sciences, Air Force Office of Scientific Research, Grant No. 77-3293.

References and Notes

(1) P. J. Flory and R. S. Frost, *Macromolecules*, companion paper in this issue, part 3.
(2) P. J. Flory, "Principles of Polymer Chemistry", Cornell University Press, Ithaca, N.Y., 1953, pp 336–9.
(3) P. J. Flory and A. Abe, *Macromolecules*, companion paper in this issue, part 1.
(4) P. J. Flory, *Proc. R. Soc. London, Ser A*, **234**, 73 (1956).

Statistical Thermodynamics of Mixtures of Rodlike Particles. 5. Mixtures with Random Coils

Paul J. Flory

Department of Chemistry, Stanford University, Stanford, California 94305.
Received June 8, 1978

ABSTRACT: Ternary systems consisting of a solvent (1), a rigid rod solute (2), and a randomly coiled polymer chain (3) are treated according to the model and procedures employed in part 1. Phase equilibria are calculated for systems specified by (x_2,x_3) = (10,10), (20,20), (20,∞), and (100,100), where x_2 and x_3 are the molar volumes of the respective solutes relative to the solvent. Addition of component 3 to the binary system 1,2 increases the volume fraction v_2' of the rodlike solute in the anisotropic phase and broadens the biphasic gap. The preponderance of component 3 is retained by the isotropic phase. Its volume fraction v_3' in the anisotropic phase is $<10^{-4}$ for all compositions and becomes vanishingly small if v_2' is much increased by raising v_3 in the isotropic phase. The isotropic phase exhibits a somewhat greater tolerance for the rodlike component (2). For large values of x_2 and v_3, however, v_2 becomes negligible. The marked segregation of these components between the two phases underscores the basic differences in their mixing tendencies.

Ternary systems comprising an isodiametrical solvent (1), a rodlike solute (2), and a random-coiled chain (3) are considered in this paper. The diameters of components 2 and 3 are assumed equal to that of the solvent. The axis ratio of 2 is x_2 and the contour length of 3 is x_3; i.e., the molecular volumes of the components are in the ratio $1:x_2:x_3$. The theory elaborated in part 1[1] of this series is readily adapted to systems of this description.

The solutes of the ternary systems treated in this paper represent extremes. The one consists of rigid particles of well-defined geometrical form and the other of molecules possessing a substantial degree of flexibility, which therefore assume highly irregular spatial configurations. The profound differences in their mixing behavior are reflected in their limited compatibility with one another. Partitioning of the solute components between nematic and isotropic phases in equilibrium is reminiscent of the "fractionation" of the pairs of rodlike solutes differing in axis ratio considered in paper 2.[2] It is even more marked, however, than for the systems encountered in 2.

Again, the treatment is restricted to "athermal" mixtures or, stated more precisely, to systems in which the exchange free energy is null.

Theory

Combinatorial analysis of the ternary system identified above by use of the lattice model along the lines followed in 1[1,3] yields for the mixing partition function

$$Z_M = \left\{\frac{[n_0 - n_2(x_2 - y)]!y^{2n_2}}{(n_0 - x_2n_2)!n_2!n_0^{n_2(y-1)}}\right\} \times \left\{\frac{(n_0 - x_2n_2)!z_3^{n_3}}{(n_0 - x_2n_2 - x_3n_3)!n_3!n_0^{n_3(x_3-1)}}\right\} \quad (1)$$

$$Z_M = \frac{[n_0 - n_2(x_2 - y)]!y^{2n_2}z_3^{n_3}}{n_1!n_2!n_3!n_0^{n_2(y-1)+n_3(x_3-1)}} \quad (2)$$

where

$$n_0 = n_1 + n_2x_2 + n_3x_3 \quad (3)$$

and z_3 is the internal configuration partition function for the ramdon coil. The first factor in braces in eq 1 expresses the expected number of configurations for the rodlike species in the empty lattice. It corresponds to eq 1-8 as applied to a monodisperse solute. The second term in eq 1 takes account of the configurations accessible to the n_3 random coils subsequently added to the lattice. Introduction of Stirling's approximations for the factorials leads to

$$-\ln Z_M = n_1 \ln v_1 + n_2 \ln v_2 + n_3 \ln v_3 - n_0[1 - v_2(1 - y/x_2)] \ln [1 - v_2(1 - y/x_2)] + n_2(y - 1) - n_2 \ln (x_2y^2) + n_3(x_3 - 1) - n_3 \ln (x_3z_3)] \quad (4)$$

where v_1, v_2, and v_3 are the volume fractions of the respective components.

0024-9297/78/2211-1138$01.00/0

Equating $\partial Z_M/\partial y$ to zero, one obtains

$$\exp(-2/y) = 1 - v_2(1 - y/x_2) \quad (5)$$

(compare eq 1-12) where y is the mean value of the disorder index at equilibrium.

The chemical potentials that follow from eq 4 are given by

$$(\mu_1 - \mu_1^0)/RT = \ln v_1 + v_2(y - 1)/x_2 + v_3(1 - 1/x_3) - \ln [1 - v_2(1 - y/x_2)] \quad (6)$$

$$(\mu_2 - \mu_2^0)/RT = \ln (v_2/x_2) + v_2(y - 1) + v_3x_2(1 - 1/x_3) - y \ln [1 - v_2(1 - y/x_2)] - 2 \ln y \quad (7)$$

$$(\mu_3 - \mu_3^0)/RT = \ln (v_3/x_3) + v_2(x_3/x_2)(y - 1) + v_3(x_3 - 1) - x_3 \ln [1 - v_2(1 - y/x_2)] - \ln z_3 \quad (8)$$

where y is understood to assume its equilibrium value given by eq 5. Substitution from eq 5 in each of these equations yields

$$(\mu_1 - \mu_1^0)/RT = \ln v_1 + v_2(y - 1)/x_2 + v_3(1 - 1/x_3) + 2/y \quad (9)$$

$$(\mu_2 - \mu_2^0)/RT = \ln (v_2/x_2) + v_2(y - 1) + v_3x_2(1 - 1/x_3) + 2(1 - \ln y) \quad (10)$$

$$(\mu_3 - \mu_3^0)/RT = \ln (v_3/x_3) + v_2(x_3/x_2)(y - 1) + v_3(x_3 - 1) + 2x_3/y - \ln z_3 \quad (11)$$

The chemical potentials for an isotropic phase are (compare eq 1-27 and -28)

$$(\mu_1 - \mu_1^0)/RT = \ln v_1 + v_2(1 - 1/x_2) + v_3(1 - 1/x_3) \quad (12)$$

$$(\mu_2 - \mu_2^0)/RT = \ln (v_2/x_2) + v_2(x_2 - 1) + v_3x_2(1 - 1/x_3) - \ln x_2^2 \quad (13)$$

$$(\mu_3 - \mu_3^0)/RT = \ln (v_3/x_3) + v_2x_3(1 - 1/x_2) + v_3(x_3 - 1) - \ln z_3 \quad (14)$$

At equilibrium between an isotropic and an anisotropic phase, one obtains by equating the chemical potentials given by eq 9, 10, and 11 in the anisotropic phase (primed) to the corresponding chemical potentials in the isotropic phase (unprimed) given by eq 12, 13, and 14, respectively,

$$\ln (v_1'/v_1) = A - B - 2/y \quad (15)$$

$$\ln (v_2'/v_2) = (A - B)x_2 - 2 \ln (x_2e/y) \quad (16)$$

$$\ln (v_3'/v_3) = (A - B)x_3 - 2x_3/y \quad (17)$$

where

$$A = v_2(1 - 1/x_2) + v_3(1 - 1/x_3) \quad (18)$$

and

$$B = v_2'(y - 1)/x_2 + v_3'(1 - 1/x_3) \quad (19)$$

Elimination of $A - B$ by combination of eq 17 with 16 gives

$$\ln (v_2'/v_2) - (x_2/x_3) \ln (v_3'/v_3) = 2x_2/y - 2 \ln (x_2e/y) \quad (20)$$

For given x_2, x_3, and v_2', these equations may be solved for y, v_3', v_2, and v_3 as follows. We first obtain y from eq 5 with v_2 therein replaced by v_2'. Choice of trial values for v_2 and v_3 permits evaluation of A according to eq 18, and of v_3' by use of eq 20. Substitution of y, v_2', and v_3' in eq 19 gives B. Equation 16 may then be used to obtain a value for v_2 with which to replace the trial v_2. The value of v_2 that is consistent with the chosen v_3 may then be determined by iteration. Substitution of $v_1' = 1 - v_2' - v_3'$ in eq 15 yields a value of v_1 which may be compared with $v_1 = 1 - v_2 - v_3$. A new value of v_3 may then be chosen and the procedure repeated, and so forth until a satisfactory solution is obtained.

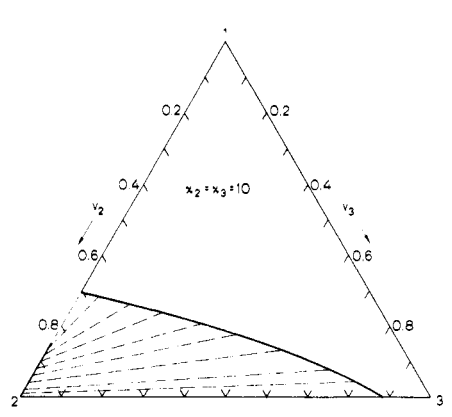

Figure 1. Phase diagram for the system with $x_2 = x_3 = 10$. Components are solvent (1), rigid rod solute (2), and random coil (3). Binodials are shown as heavy lines. The binodial for the anisotropic phase does not depart perceptibly from the 1,3 axis. Tie lines are light dashed.

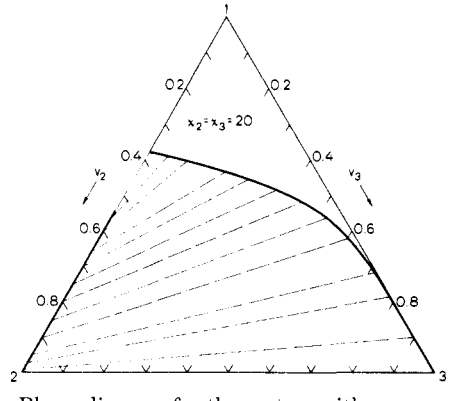

Figure 2. Phase diagram for the system with $x_2 = x_3 = 20$. See legend to Figure 1.

For an undiluted binary mixture of the macromolecular components 2 and 3, i.e., for $v_1 = 0$, eq 15 requires that $v_1' = 0$ also. Equations 16 and 17 reduce in this case to

$$\ln (v_2'/v_2) = v_2'(x_2 - y) + (v_2' - v_2)(1 - x_2/x_3) - 2 \ln (x_2e/y) \quad (21)$$

and to

$$\ln (v_3'/v_3) = [\ln (1 - v_2')/(1 - v_2)] = (x_3/x_2)[v_2'(x_2 - y) + (v_2' - v_2)(1 - x_2/x_3)] - 2x_3/y \quad (22)$$

respectively. For given x_2 and x_3, eq 21 and 22, in conjunction with eq 5, may be solved simultaneously for v_2 and v_2' and, hence, for $v_3 = 1 - v_2$ and $v_3' = 1 - v_2'$ as well.

Numerical Calculations

Phase diagrams calculated by the methods above are presented in Figures 1, 2, and 4 for ternary systems with $x_2 = x_3 = 10$, 20, and 100, respectively. The phase diagram calculated for the system with $x_2 = 20$ and $x_3 = \infty$ is shown in Figure 3. Binodials for the isotropic and anisotropic phases are heavy lined. Tie lines joining conjugate phases in equilibrium are light dashed. Full ranges of the volume fractions are shown in Figures 1, 2, and 3. Only the upper portion of the phase diagram for $x_2 = 100$, within which $(1 - v_1) < 0.20$, is included in Figure 4. Values of v_2' for the lower termini of tie lines truncated by the base line of this diagram are recorded on the tie lines. Additional calculations for the systems $x_2 = x_3 = 7$ and $x_2 = 20$, $x_3 =$

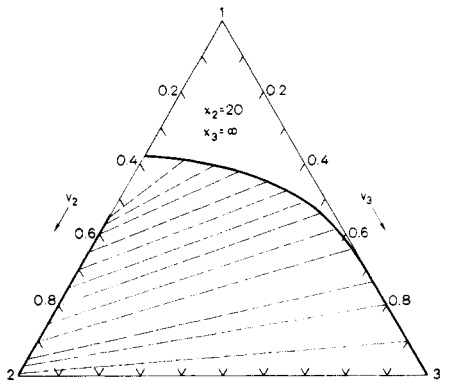

Figure 3. Phase diagram for the system with $x_2 = 20$ and $x_3 = \infty$. See legend to Figure 1.

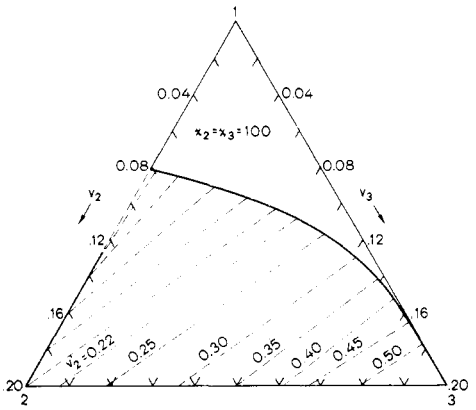

Figure 4. Portion of the phase diagram for the system with $x_2 = x_3 = 100$ within which $v_2 + v_3 < 0.20$. See legend to Figure 1. Numerals on tie lines that extend beyond the lower boundary of this diagram denote v_2' at the terminus of the tie line on the binodial for the nematic phase.

100 reveal no features beyond those that may be inferred from the results shown. Hence, they have not been included.

Commencing with the binary system consisting of diluent (1) and rodlike solute (2), we observe that incorporation of the random coil component (3) in the isotropic phase brings about a relatively small increase in the combined concentration of solutes $(1 - v_1)$ in that phase, as indicated by the downward slopes of the binodials in Figures 1–4. This slope is especially small in the case $x_3 = \infty$ shown in Figure 3. In every case the greater part of the random-coiled component added, commencing with the binary system 1,2, replaces component 2, rather than component 1, in the isotropic phase. Simultaneously, the solute concentration in the conjugate nematic phase increases substantially. Little of component 3 enters this phase, however, its proportions therein being too small to be discernible in Figures 1, 2, and 4; i.e., the binodials for the nematic phases depart imperceptibly from the 1,2 axes. In the system $x_2 = 20$, $x_3 = \infty$ shown in Figure 3 this component is of course excluded altogether from the nematic phase.

The volume fractions v_3' along the binodial for the nematic phases in the systems with $x = 10$ and 20 are plotted on an expanded scale against v_2' in Figure 5. The curves rise sharply from the points at v_2' for the binary systems 1,2. They pass through maxima, then fall rapidly toward zero with further increase in v_2', i.e., with passage downward along the nematic binodials in Figures 1 and 2. Even at the maxima, v_3' is only ca. 0.5×10^{-4}. As v_2' is increased beyond the maximum, v_3' decreases rapidly, becoming vanishingly small as the concentration of solutes

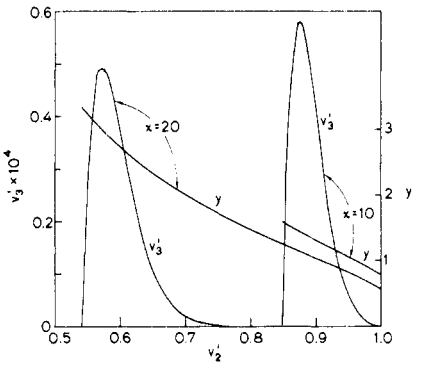

Figure 5. Volume fractions v_3' of random coil in the anisotropic phase plotted against v_2' for the rodlike solute in that phase for $x_2 = x_3 = x = 10$ and 20. Values of y also are shown.

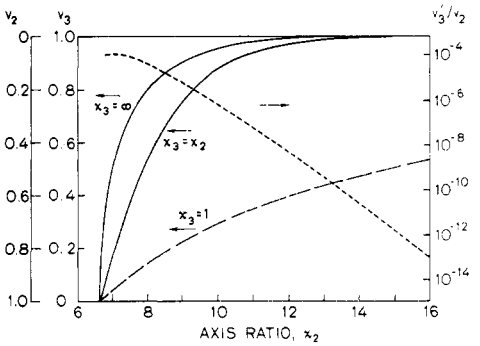

Figure 6. Phase compositions for binary systems 2,3 ($v_1 = 0$). Solid lines represent the volume fractions v_3 of the random coil in the isotropic phase at equilibrium as functions of the axis ratio x_2 of the rodlike component: the upper solid curve, $x_3 = \infty$; lower solid curve, $x_3 = x_2$. The long dashed curve is for $x_3 = 1$. The short dashed curve represents $v_3'/v_2 = v_3'/(1 - v_3)$ for systems with $x_3 = x_2$, plotted on the logarithmic scale on the right.

in the nematic phase approaches unity. At $v_1' = 0$, for example, $v_3' = 8 \times 10^{-8}$ for $x_2 = x_3 = 10$, and 2.4×10^{-23} for $x_2 = x_3 = 20$. Owing to the minute concentration of component 3 along the entire binodial for the nematic phase, negligible errors are incurred in all other quantities if v_3' is set equal to zero, thereby voiding the condition $\mu_3 = \mu_3'$.

Figure 3 for $x_2 = 20$, $x_3 = \infty$ resembles Figure 2 for $x_2 = x_3 = 20$. The binodial for the isotropic phase in Figure 3 follows a course somewhat above that for the system with $x_3 = 20$ shown in Figure 2; i.e., for a given ratio v_3/v_2, v_1 is *larger* in the system with $x_3 = \infty$. Tie lines for the same value of this ratio are more nearly parallel to the 2,3 base in Figure 3. This difference dominates the one first mentioned, with the result that the solvent volume fraction v_1 in the conjugate phase in Figure 3 ($x_3 = \infty$) is somewhat *lower* than in Figure 2 ($x_3 = 20$) for the same v_2'. Apart from these quantitative differences, the phase diagrams in Figures 2 and 3 are similar.

It will be observed that the downward slopes of the binodials for the isotropic phases in Figures 1–4 remain gradual until v_3/v_2 approaches unity, whereupon they curve rapidly downward. In Figures 2 and 3 for $x_2 = 20$ and in Figure 4 for $x_2 = 100$ they tend to merge with the 1,3 axis. In Figure 1 for the lowermost value of x_2, the binodial for the isotropic phase remains well removed from the 1,3 axis.

Inasmuch as components 1 and 3 are completely miscible, the binodial for the isotropic phase must invariably meet the base line at a point finitely removed from apex 3, provided of course that x_2 is finite. However, the intercept approaches $v_3 = 1$ closely for the larger values of x_2. For $x_2 = 10$ the intercept occurs at $v_2 = 1 - v_3 = 0.1191$

and for $x_2 = 20$ at 3.41×10^{-5}; for $x_2 = 100$ it is vanishingly small. These intercepts v_3 are shown as a function of x_2 by the solid curves in Figure 6 representing the binary systems 2,3 that occur when $v_1 = 0$. The upper solid curve has been calculated for $x_3 = \infty$ and the lower one for $x_3 = x_2$. The long dashed curve, included for comparison, represents the limiting case $x_3 = 1$ in which the second component is monomeric. Alternatively, this curve may be taken to represent the binary system 1,2 with component 1 designated as component 3. Each of these curves commences on the abscissa at the common point $x_2 = 6.70183$ which is the critical axis ratio for a system of one component.[3]

Comparison of the three curves for $x_3 = 1$, $x_3 = x_2$, and $x_3 = \infty$ in Figure 6 demonstrates the marked effect of chain length of the random coil component in expelling the rodlike species from the isotropic phase. At $x_2 = 10$ the respective volume fractions $v_2 = 1 - v_3$ at equilibrium are 0.7059, 0.1191, and 0.0459. At $x_2 = 15$ they are 0.4925, 2.400×10^{-3}, and 0.883×10^{-3}. For $x_2 \geq 20$ and $x_3 \geq x_2$ the volume fractions v_2 are negligible.

Although, according to the calculations cited, the rejection of component 2 from the isotropic phase is pronounced even at moderate concentrations of solutes for large x_2 (see the isotropic binodial in Figure 4 at $1 - v_1 = 0.2$, for example), it is not as severe as the rejection of the random coil from the anisotropic phase. This is evident from the phase diagrams for the ternary systems shown in Figures 1–4. It is demonstrated further by the declining dashed curve in Figure 6 showing v_3'/v_2, or $v_3'/(1 - v_3)$, plotted on the logarithmic scale along the right-hand ordinate as a function of x_2 for the binary systems 2,3 in which $x_3 = x_2$. Thus, as $x_2 = x_3$ increases, v_2 in the isotropic phase of the binary system, though very small, becomes manifoldly greater than v_3' in the conjugate nematic phase.

The severity of the preferential partitioning of the respective solutes between the two phases in the ternary systems is shown further by the inclinations of the tie lines in Figures 1–4 to the straight lines (not shown) extending from apex 1 through the tie line termini on the binodial for the isotropic phase. Thus, the ratio v_3/v_2 for the isotropic phase is much greater than v_3'/v_2' for its nematic conjugate phase. Although this feature is more pronounced the larger the value of x_2, it is conspicuous even at $x_2 = 10$. As noted above, it is accentuated by an increase in x_3.

Discussion

The marked discrimination between the disparate solute species by the coexisting isotropic and anisotropic phases clearly is the most striking result demonstrated by the calculations presented above. The two solute species considered represent extremes, the one being rigid and rodlike and the other sufficiently flexible to adopt a random-coiled configuration.[4] The underlying basis for the differentiation between them is manifest in the primary derivations of the configuration partition function.[1,3] The diverse behaviors can be traced through the terms in y appearing in the chemical potentials for the anisotropic phase (see eq 9–11) and comparison with their counterparts for the isotropic phase (see eq 12–14). From a physical point of view, the isotropic phase offers to a rodlike solute none of the advantages of orientation. Hence, this component prefers the anisotropic phase where obstruction by neighboring species is alleviated by mutual alignment. To an even greater degree, intrusion of the random coil into the anisotropic phase tends to impose overlaps that are not mitigated by the prevailing orientation.

The anisotropic phase approaches the selectivity of a pure crystal in its rejection of a foreign component, in this case the random coil. For a large axis ratio (e.g., for $x_2 = x_3 = 100$) a high degree of selectivity occurs even at relatively low concentrations, where the volume fraction of solvent exceeds that of the rodlike solute severalfold.

The results of this investigation have obvious implications with reference to helix–coil transitions at concentrations conducive to separation of a nematic phase.

Acknowledgment. This work was supported by the Directorate of Chemical Sciences, Air Force Office of Scientific Research, Grant No. 77-3293.

References and Notes

(1) P. J. Flory and A. Abe, *Macromolecules*, companion paper in this issue, part 1.
(2) A. Abe and P. J. Flory, *Macromolecules*, companion paper in this issue, part 2.
(3) P. J. Flory, *Proc. R. Soc., London, Ser. A*, **234**, 60 (1956).
(4) P. J. Flory, *Pure Appl. Chem., Macromol. Chem.*, **8**, 1–15 (1972); P. J. Flory, *J. Macromol. Sci., Phys.*, **B12** (1), 1–11 (1976).

Statistical Thermodynamics of Mixtures of Rodlike Particles. 6. Rods Connected by Flexible Joints

Paul J. Flory

Department of Chemistry, Stanford University, Stanford, California 94305.
Received June 8, 1978

ABSTRACT: Solutions are treated in which the solute molecule comprises m rodlike sequences, each of axis ratio x, connected in linear succession by $m - 1$ joints permitting free orientations. Separation of an anisotropic phase depends predominantly on x. Increasing the chain length from x to $x_m = mx$ by joining m rods affects the compositions of the phases coexisting at equilibrium by only a few percent. The implications of these results on the behavior to be expected in systems of semirigid real chains of various types are discussed.

Chain molecules, however constituted, invariably possess some degree of flexibility. Even in instances, exemplified by poly(*p*-phenylene), where the skeletal bonds are nominally collinear, bending of bond angles must introduce a finite degree of flexibility. Stable helical conformations, such as those of the polypeptide α helix and of double-stranded DNA, likewise are subject to small, random departures of their helical axes from strict rectilinearity. The cumulative effect of these deviations throughout a very long chain may be substantial. In particular, the

0024-9297/78/2211-1141$01.00/0